

g factor of Li-like ions with nonzero nuclear spin

D. L. Moskovkin¹, V. M. Shabaev¹, and W. Quint²

¹*Department of Physics, St. Petersburg State University, Oulianovskaya 1, Petrodvorets,
St. Petersburg 198504, Russia*

²*Gesellschaft für Schwerionenforschung, Planckstrasse 1, D-64291 Darmstadt, Germany*

Abstract

The fully relativistic theory of the *g* factor of Li-like ions with nonzero nuclear spin is considered for the $(1s)^2 2s$ state. The magnetic-dipole hyperfine-interaction correction to the atomic *g* factor is calculated including the one-electron contributions as well as the interelectronic-interaction effects of order $1/Z$. This correction is combined with the interelectronic-interaction, QED, nuclear recoil, and nuclear size corrections to obtain high-precision theoretical values for the *g* factor of Li-like ions with nonzero nuclear spin. The results can be used for a precise determination of nuclear magnetic moments from *g* factor experiments.

PACS number(s): 31.30.Jv, 31.30.Gs, 32.60.+i, 12.20.Ds

1 Introduction

Recent measurements of the *g* factor of hydrogenlike carbon and oxygen have reached an accuracy of about $2 \cdot 10^{-9}$ [1–3]. These experiments stimulated theoretical investigations of this effect [4–21]. Besides a new possibility for tests of the magnetic sector of quantum electrodynamics (QED), these investigations have already provided a new determination of the electron mass (see Refs. [3, 22] and references therein). Extensions of these measurements to systems with higher nuclear charge number Z and to ions with nonzero nuclear spin would also provide the basis for new determinations of the fine-structure constant [8, 22–24], the nuclear magnetic moments [23], and the nuclear charge radii. Investigations of the transition probability between the hyperfine-structure components in hydrogenlike bismuth [25–28] clearly indicated the importance of the QED correction to the *g* factor for agreement between theory and experiment.

Extending theoretical description from H-like to Li-like ions, one encounters a serious complication due to the presence of additional electrons. A number of relativistic calculations of the *g* factor of Li-like ions were carried out previously [29–34]. However, to reach the accuracy comparable to the one for H-like ions, a systematic quantum electrodynamic (QED) treatment is required [16, 35–38]. In the present paper, we consider the *g* factor of lithiumlike ions with nonzero nuclear spin. Calculations of the *g* factor for these ions should include corrections depending on the nuclear *g* factor. Besides a simple lowest-order nuclear-spin-dependent contribution, one should calculate the hyperfine-interaction correction, including the interelectronic-interaction effects. In the present paper, the magnetic-dipole hyperfine-structure correction is calculated in a wide range of the nuclear charge number $Z = 3 – 100$. The electric-quadrupole hyperfine-structure correction is evaluated as well. The calculations are based on perturbation theory in the parameter $1/Z$. The contributions of zeroth and first orders in $1/Z$ are taken into account for the magnetic-dipole correction and the contribution of zeroth order is taken into consideration for the electric-quadrupole one. The $1/Z$ correction is evaluated within a rigorous QED approach. The obtained results are

combined with the other corrections to get accurate theoretical predictions for the g factor of lithiumlike ions with nonzero nuclear spin.

Experimental investigations in this direction are anticipated in the near future at University of Mainz and GSI [39].

Relativistic units ($\hbar = c = 1$) and the Heaviside charge unit ($\alpha = e^2/4\pi$, $e < 0$) are used in the paper. In some important cases, the final formulas contain \hbar and c explicitly to be applicable for arbitrary system of units.

2 The g factor in the lowest-order one-electron approximation

We consider a lithiumlike ion placed in a weak homogeneous magnetic field \vec{B} directed along the z axis. Assuming that the energy level shift (splitting) due to interaction of the valent $2s$ electron with \vec{B} is much smaller than the hyperfine-structure splitting, $\Delta E_{\text{mag}} \ll \Delta E_{\text{HFS}}$, we can express the linear-dependent part of this shift in terms of the g factor,

$$\Delta E_{\text{mag}} = g\mu_0 B M_F, \quad (1)$$

where M_F is the z projection of the total atomic angular momentum $F = j+I, j+I-1, \dots, |j-I|$; $M_F = -F, -F+1, \dots, F-1, F$; j and I are the total electron and nuclear angular momenta, respectively; $\mu_0 = |e|/(2m_e c)$ is the Bohr magneton. To obtain g in relativistic approximation to the lowest order, we have to evaluate the expression

$$\Delta E_{\text{mag}} = \langle nljIMF | V_{\vec{B}} | nljIMF \rangle, \quad (2)$$

where

$$V_{\vec{B}} = V_{\vec{B}}^{(e)} + V_{\vec{B}}^{(n)}, \quad (3)$$

$$V_{\vec{B}}^{(e)} = -e(\vec{\alpha} \cdot \vec{A}) = \frac{|e|}{2}(\vec{\alpha} \cdot [\vec{B} \times \vec{r}]), \quad (4)$$

the vector $\vec{\alpha}$ incorporates the Dirac α matrices, and

$$V_{\vec{B}}^{(n)} = -(\vec{\mu} \cdot \vec{B}). \quad (5)$$

Here $V_{\vec{B}}^{(e)}$ describes the interaction of the valent electron with the homogeneous magnetic field and $V_{\vec{B}}^{(n)}$ describes the interaction of the nuclear magnetic moment $\vec{\mu}$ with \vec{B} . $|nljIMF\rangle$ is the atomic wave function that corresponds to given values of F and M_F . It is a linear combination of products of electron and nuclear wave functions:

$$|nljIMF\rangle = \sum_{m_j, M_I} C_{jm_j IM_I}^{FM_F} |nljm_j\rangle |IM_I\rangle. \quad (6)$$

Here $C_{jm_j IM_I}^{FM_F}$ are the Clebsch-Gordan coefficients; $|nljm_j\rangle$ are the unperturbed one-electron wave functions, which are four-component eigenvectors of the Dirac equation for the Coulomb field, with the total angular momentum j and its projection m_j ; n is the principal quantum number and $l = j \pm \frac{1}{2}$ defines the parity of the state. $|IM_I\rangle$ are the nuclear wave functions with the total angular momentum I and its projection M_I .

In what follows, we adopt for the nuclear magnetic moment $\mu = \langle II|\mu_z|II\rangle$, where μ_z is the z projection of the nuclear magnetic moment operator $\vec{\mu}$ acting in the space of nuclear wave functions $|IM_I\rangle$.

A simple integration over the angular variables in Eq. (2) yields the well-known result (see, e.g., Ref. [40])

$$g = g_D \frac{F(F+1) + j(j+1) - I(I+1)}{2F(F+1)} - \frac{m_e}{m_p} g_I \frac{F(F+1) + I(I+1) - j(j+1)}{2F(F+1)}. \quad (7)$$

Here m_e and m_p are the electron and the proton mass, respectively, g_D is the one-electron Dirac value of the ground-state g factor of the lithium-like ion, $g_I = \mu/(\mu_N I)$ is the nuclear g factor, and $\mu_N = |e|/(2m_p c)$ is the nuclear magneton. To obtain g_D we have to calculate $\langle nljm_j|V_{\vec{B}}^{(e)}|nljm_j\rangle$. For the point-nucleus case, a simple evaluation for the $2s$ state yields

$$g_D = \frac{2[\sqrt{2+2\gamma} + 1]}{3} = 2 - \frac{(\alpha Z)^2}{6} + \dots, \quad (8)$$

where $\gamma = \sqrt{1 - (\alpha Z)^2}$.

The g_I -dependent term in the right-hand side of equation (7) is by a factor $m_e/m_p \approx 1/1836$ smaller than the first term. However, since it is much larger than the current experimental uncertainty, this equation can be used for determination of g_I from the g -factor experiments, provided all the corrections to expression (7) are calculated to a high accuracy or are known from the corresponding experiment for another isotope of the same element. In particular, to meet the level of the current experimental accuracy, we need to evaluate the hyperfine-interaction correction.

3 Hyperfine-interaction corrections

The hyperfine-interaction operator is given by the sum

$$V_{\text{HFS}} = V_{\text{HFS}}^{(\mu)} + V_{\text{HFS}}^{(Q)}, \quad (9)$$

where $V_{\text{HFS}}^{(\mu)}$ and $V_{\text{HFS}}^{(Q)}$ are the magnetic-dipole and electric-quadrupole hyperfine-interaction operators, respectively. In the point-dipole approximation,

$$V_{\text{HFS}}^{(\mu)} = \frac{|e|}{4\pi} \frac{(\vec{\alpha} \cdot [\vec{\mu} \times \vec{r}])}{r^3}, \quad (10)$$

and, in the point-quadrupole approximation,

$$V_{\text{HFS}}^{(Q)} = -\alpha \sum_{m=-2}^{m=2} Q_{2m} \eta_{2m}^*(\vec{n}). \quad (11)$$

Here $Q_{2m} = \sum_{i=1}^Z r_i^2 C_{2m}(\vec{n}_i)$ is the operator of the electric-quadrupole moment of the nucleus, $\eta_{2m} = C_{2m}(\vec{n})/r^3$ is an operator that acts on electron variables, $\vec{n} = \vec{r}/r$, $\vec{n}_i = \vec{r}_i/r_i$, \vec{r} is the position vector of the electron, \vec{r}_i is the position vector of the i -th proton in the nucleus, $C_{lm} = \sqrt{4\pi/(2l+1)} Y_{lm}$, and Y_{lm} is a spherical harmonic. It must be stressed that the electric-quadrupole interaction should be taken into account only for ions with $I > 1/2$.

In the one-electron approximation, the magnetic-dipole and electric-quadrupole hyperfine-interaction corrections to the ground-state g factor of the Li-like ion are given by

$$\delta g_{\text{HFS}(\mu, Q)}^{\text{one-el.}(2s)} = \frac{2}{\mu_0 B M_F} \sum_{m_j M_I} \sum_{m'_j M'_I} C_{\frac{1}{2} m_j I M_I}^{F M_F} C_{\frac{1}{2} m'_j I M'_I}^{F M_F} \langle I M_I | \sum_n^{\langle \varepsilon_n \neq \varepsilon_v \rangle} \frac{\langle v | V_{\vec{B}}^{(e)} | n \rangle \langle n | V_{\text{HFS}}^{(\mu, Q)} | v' \rangle}{\varepsilon_v - \varepsilon_n} | I M'_I \rangle, \quad (12)$$

where $|v\rangle = |20\frac{1}{2}m_j\rangle$ and $|v'\rangle = |20\frac{1}{2}m'_j\rangle$ are the $2s$ states of the valent electron with the angular momentum projections m_j and m'_j , respectively, $|n\rangle \equiv |nljm_j\rangle$, $\varepsilon_v = \varepsilon_{2s}$ and ε_n are the one-electron Dirac energies in the Coulomb field of the nucleus. The summation in (12) runs over discrete as well as continuum states. The corresponding diagrams are presented in Fig. 1.

The total hyperfine-interaction correction to the ground-state g factor of the Li-like ion is given by

$$\delta g_{\text{HFS}}^{(2s)} = \delta g_{\text{HFS}(\mu)}^{(2s)} + \delta g_{\text{HFS}(Q)}^{(2s)} \quad (13)$$

with

$$\delta g_{\text{HFS}(\mu)}^{(2s)} = \alpha^2 Z \frac{1}{12} \frac{\mu}{\mu_N} \frac{m_e}{m_p} \frac{1}{I} Y_{\text{nuc}}^{(\mu)}(F) [S_2(\alpha Z) + \frac{1}{Z} B_\mu(\alpha Z) + \frac{1}{Z^2} C_\mu(\alpha Z) + \dots] \quad (14)$$

and

$$\delta g_{\text{HFS}(Q)}^{(2s)} = \alpha^4 Z^3 \frac{23}{2160} Q \left(\frac{m_e c}{\hbar} \right)^2 Y_{\text{nuc}}^{(Q)}(F) [T_2(\alpha Z) + \frac{1}{Z} B_Q(\alpha Z) + \frac{1}{Z^2} C_Q(\alpha Z) + \dots]. \quad (15)$$

Here the angular factors are

$$Y_{\text{nuc}}^{(\mu)}(F) = \frac{F(F+1) + I(I+1) - 3/4}{2F(F+1)} = \begin{cases} \frac{2(I+1)}{2I+1} & \text{for } F = I - \frac{1}{2} \\ \frac{2I}{2I+1} & \text{for } F = I + \frac{1}{2} \end{cases} \quad (16)$$

and

$$Y_{\text{nuc}}^{(Q)}(F) = \begin{cases} -\frac{(I+1)(2I+3)}{I(2I-1)(2I+1)} & \text{for } F = I - \frac{1}{2} \\ \frac{1}{2I+1} & \text{for } F = I + \frac{1}{2} \end{cases}, \quad (17)$$

and $Q = 2\langle II|Q_{20}|II\rangle$ is the electric-quadrupole moment of the nucleus. The functions

$$S_2(\alpha Z) = \frac{12}{\alpha^2 Z \frac{m_e}{m_p} g_I Y_{\text{nuc}}^{(\mu)}(F)} \delta g_{\text{HFS}(\mu)}^{\text{one-el.}(2s)} \quad (18)$$

and

$$T_2(\alpha Z) = \frac{2160}{23\alpha^4 Z^3 Q \left(\frac{m_e c}{\hbar} \right)^2 Y_{\text{nuc}}^{(Q)}(F)} \delta g_{\text{HFS}(Q)}^{\text{one-el.}(2s)} \quad (19)$$

determine the one-electron contributions, which are discussed in detail in Ref. [20]. For the point-charge nucleus, the functions $S_2(\alpha Z)$ and $T_2(\alpha Z)$ are [20]

$$\begin{aligned} S_2(\alpha Z) &= \frac{8}{3N} \left\{ \frac{1}{N+2} \left[N + \frac{10(N+1)}{3N} \right] + \frac{(\alpha Z)^2}{\gamma(\gamma+1)} \left[\frac{2(N+1)}{3-4(\alpha Z)^2} + 1 \right] - \frac{1}{\gamma} \right\} \\ &= 1 + \frac{229}{144} (\alpha Z)^2 + \dots \end{aligned} \quad (20)$$

and

$$\begin{aligned} T_2(\alpha Z) &= \frac{192[(N + \gamma + 1)\{18 + 24\gamma - 12N + 8\gamma N^2\} + 15(1 + \gamma)]}{23\gamma N^3[15 - 16(\alpha Z)^2](N + \gamma + 1)^2} \\ &= 1 + \frac{427}{276}(\alpha Z)^2 + \dots, \end{aligned} \quad (21)$$

where $N = \sqrt{2(1 + \gamma)}$.

The interelectronic-interaction correction $B_\mu(\alpha Z)$ is calculated within the rigorous QED approach. The interaction of the electrons with the Coulomb field of the nucleus is included in the unperturbed Hamiltonian, i.e. the Furry picture is used. The perturbation theory is formulated with the technique of the two-time Green function (TTGF) [26]. To simplify the calculations, the closed $(1s)^2$ shell is regarded as belonging to a redefined vacuum. With this vacuum, the Fourier transform of TTGF can be introduced by

$$\begin{aligned} \mathcal{G}(E; \vec{x}; \vec{x}')\delta(E - E') &= \frac{1}{2\pi i} \int_{-\infty}^{\infty} dx^0 dx'^0 \exp(iE'x'^0 - iEx^0) \\ &\times \langle 0_{(1s)^2} | T\psi(x'^0, \vec{x}')\psi^\dagger(x^0, \vec{x}) | 0_{(1s)^2} \rangle, \end{aligned} \quad (22)$$

where $\psi(x^0, \vec{x})$ is the electron-positron field operator in the Heisenberg representation and T is the time-ordered product operator. The energy shift of a state a can be expressed in terms of the TTGF defined by

$$g_{aa}(E) = \langle u_a | \mathcal{G}(E) | u_a \rangle \equiv \int d\vec{x} d\vec{x}' u_a^\dagger(\vec{x}') \mathcal{G}(E; \vec{x}'; \vec{x}) u_a(\vec{x}), \quad (23)$$

where $u_a(\vec{x})$ is the unperturbed Dirac wave function of the state a . Using the Sz.-Nagy and Kato technique [41], one can derive for the total energy shift $\Delta E_a \equiv E_a - E_a^{(0)}$ [26, 42]

$$\Delta E_a = \frac{\frac{1}{2\pi i} \oint_{\Gamma} dE \Delta E \Delta g_{aa}(E)}{1 + \frac{1}{2\pi i} \oint_{\Gamma} dE \Delta g_{aa}(E)}, \quad (24)$$

where $\Delta E = E - E_a^{(0)}$, $\Delta g_{aa}(E) \equiv g_{aa}(E) - g_{aa}^{(0)}(E)$, and $g_{aa}^{(0)}(E) = (E - E_a^{(0)})^{-1}$. The contour integrals in the complex E -plane are taken along the contour Γ which surrounds the pole of $g_{aa}(E)$ corresponding to the level a and keeps outside all other singularities. The contour Γ is oriented counter-clockwise.

To first three orders of the perturbation theory, the energy shift is given by

$$\Delta E_a^{(1)} = \frac{1}{2\pi i} \oint_{\Gamma} dE \Delta E \Delta g_{aa}^{(1)}(E), \quad (25)$$

$$\Delta E_a^{(2)} = \frac{1}{2\pi i} \oint_{\Gamma} dE \Delta E \Delta g_{aa}^{(2)}(E) - \left(\frac{1}{2\pi i} \oint_{\Gamma} dE \Delta E \Delta g_{aa}^{(1)}(E) \right) \left(\frac{1}{2\pi i} \oint_{\Gamma} dE \Delta g_{aa}^{(1)}(E) \right), \quad (26)$$

$$\begin{aligned} \Delta E_a^{(3)} &= \frac{1}{2\pi i} \oint_{\Gamma} dE \Delta E \Delta g_{aa}^{(3)}(E) - \left(\frac{1}{2\pi i} \oint_{\Gamma} dE \Delta E \Delta g_{aa}^{(2)}(E) \right) \left(\frac{1}{2\pi i} \oint_{\Gamma} dE \Delta g_{aa}^{(1)}(E) \right) \\ &- \left(\frac{1}{2\pi i} \oint_{\Gamma} dE \Delta E \Delta g_{aa}^{(1)}(E) \right) \left(\frac{1}{2\pi i} \oint_{\Gamma} dE \Delta g_{aa}^{(2)}(E) \right) \\ &+ \left(\frac{1}{2\pi i} \oint_{\Gamma} dE \Delta E \Delta g_{aa}^{(1)}(E) \right) \left(\frac{1}{2\pi i} \oint_{\Gamma} dE \Delta g_{aa}^{(1)}(E) \right)^2. \end{aligned} \quad (27)$$

The redefinition of the vacuum changes $i0$ to $-i0$ in the electron propagator denominators corresponding to the closed $(1s)^2$ shell. In other words it means replacing the standard Feynman contour of integration over the electron energy C with a new contour C' (Fig. 2). The second-order contribution is defined by the diagrams presented in Fig. 1. Its evaluation according to Eq. (26) yields formula (12). In the formalism under consideration, the lowest-order interelectronic-interaction and the radiative corrections to Eq. (12) are described by the third-order diagrams presented in Fig. 3 and, according to Eq. (27), by some products of the low-order diagrams depicted in Figs. 4 and 5. According to Fig. 2, to separate the interelectronic-interaction corrections, the contour C' must be divided into two parts, C and C_{int} . The integral along the standard Feynman contour C gives the one-electron radiative correction. The integral along the contour C_{int} describes the interaction of the valent electron with the closed shell electrons. Its evaluation in the Feynman gauge employing formula (27) yields for the interelectronic-interaction correction $B_\mu(\alpha Z)$

$$B_\mu(\alpha Z) = \frac{12}{\alpha^2 \frac{m_e}{m_p} g_I Y_{\text{nuc}}^{(\mu)}(F)} \frac{\Delta E_{F(\mu)}^{(3)}}{\mu_0 B M_F}, \quad (28)$$

where

$$\Delta E_{F(\mu)}^{(3)} = \sum_{m_j M_I} \sum_{m'_j M'_I} C_{\frac{1}{2} m_j M_I}^{F M_F} C_{\frac{1}{2} m'_j M'_I}^{F M_F} \langle IM_I | I_\mu^{(3a)} + I_\mu^{(3b)} + I_\mu^{(3c)} + I_\mu^{(3d)} | IM'_I \rangle, \quad (29)$$

$$\begin{aligned}
I_{\mu}^{(3a)} = & \sum_{\varepsilon_c=\varepsilon_{1s}} \left(\sum_{n_1, n_2}^{(\varepsilon_{n_1} \neq \varepsilon_v, \varepsilon_{n_2} \neq \varepsilon_v)} \frac{2}{(\varepsilon_v - \varepsilon_{n_1})(\varepsilon_v - \varepsilon_{n_2})} \left[\langle v | V_{\vec{B}}^{(e)} | n_1 \rangle \langle n_1 | V_{\text{HFS}}^{(\mu)} | n_2 \rangle \langle n_2 c | I(0) | v' c \rangle \right. \right. \\
& + \langle v | V_{\vec{B}}^{(e)} | n_1 \rangle \langle n_1 c | I(0) | n_2 c \rangle \langle n_2 | V_{\text{HFS}}^{(\mu)} | v' \rangle + \langle v | V_{\text{HFS}}^{(\mu)} | n_1 \rangle \langle n_1 | V_{\vec{B}}^{(e)} | n_2 \rangle \langle n_2 c | I(0) | v' c \rangle \Big] \\
& - \sum_{\varepsilon_{\tilde{v}}=\varepsilon_v} \sum_n^{(\varepsilon_n \neq \varepsilon_v)} \frac{2}{(\varepsilon_v - \varepsilon_n)^2} \left[\langle v | V_{\vec{B}}^{(e)} | n \rangle \langle n | V_{\text{HFS}}^{(\mu)} | \tilde{v} \rangle \langle \tilde{v} c | I(0) | v' c \rangle \right. \\
& \left. \left. + \langle v | V_{\vec{B}}^{(e)} | n \rangle \langle nc | I(0) | \tilde{v} c \rangle \langle \tilde{v} | V_{\text{HFS}}^{(\mu)} | v' \rangle + \langle v | V_{\vec{B}}^{(e)} | \tilde{v} \rangle \langle \tilde{v} | V_{\text{HFS}}^{(\mu)} | n \rangle \langle nc | I(0) | v' c \rangle \right] \right), \quad (30)
\end{aligned}$$

$$\begin{aligned}
I_{\mu}^{(3b)} = & - \sum_{\varepsilon_c=\varepsilon_{1s}} \left(\sum_{n_1, n_2}^{(\varepsilon_{n_1} \neq \varepsilon_v, \varepsilon_{n_2} \neq \varepsilon_v)} \frac{2}{(\varepsilon_v - \varepsilon_{n_1})(\varepsilon_v - \varepsilon_{n_2})} \left[\langle v | V_{\vec{B}}^{(e)} | n_1 \rangle \langle n_1 | V_{\text{HFS}}^{(\mu)} | n_2 \rangle \langle n_2 c | I(\omega) | cv' \rangle \right. \right. \\
& + \langle v | V_{\vec{B}}^{(e)} | n_1 \rangle \langle n_1 c | I(\omega) | cn_2 \rangle \langle n_2 | V_{\text{HFS}}^{(\mu)} | v' \rangle + \langle v | V_{\text{HFS}}^{(\mu)} | n_1 \rangle \langle n_1 | V_{\vec{B}}^{(e)} | n_2 \rangle \langle n_2 c | I(\omega) | cv' \rangle \Big] \\
& - \sum_{\varepsilon_{\tilde{v}}=\varepsilon_v} \sum_n^{(\varepsilon_n \neq \varepsilon_v)} \frac{2}{(\varepsilon_v - \varepsilon_n)^2} \left[\langle v | V_{\vec{B}}^{(e)} | n \rangle \langle n | V_{\text{HFS}}^{(\mu)} | \tilde{v} \rangle \langle \tilde{v} c | I(\omega) | cv' \rangle \right. \\
& \left. + \langle v | V_{\vec{B}}^{(e)} | n \rangle \langle nc | I(\omega) | c\tilde{v} \rangle \langle \tilde{v} | V_{\text{HFS}}^{(\mu)} | v' \rangle + \langle v | V_{\vec{B}}^{(e)} | \tilde{v} \rangle \langle \tilde{v} | V_{\text{HFS}}^{(\mu)} | n \rangle \langle nc | I(\omega) | cv' \rangle \right] \\
& + \sum_{\varepsilon_{\tilde{v}}=\varepsilon_v} \sum_n^{(\varepsilon_n \neq \varepsilon_v)} \frac{2}{\varepsilon_v - \varepsilon_n} \left[\langle v | V_{\vec{B}}^{(e)} | n \rangle \langle n | V_{\text{HFS}}^{(\mu)} | \tilde{v} \rangle \langle \tilde{v} c | I'(\omega) | cv' \rangle \right. \\
& \left. + \langle v | V_{\vec{B}}^{(e)} | n \rangle \langle nc | I'(\omega) | c\tilde{v} \rangle \langle \tilde{v} | V_{\text{HFS}}^{(\mu)} | v' \rangle + \langle v | V_{\vec{B}}^{(e)} | \tilde{v} \rangle \langle \tilde{v} | V_{\text{HFS}}^{(\mu)} | n \rangle \langle nc | I'(\omega) | cv' \rangle \right] \\
& + \sum_{\varepsilon_{\tilde{v}}=\varepsilon_v} \sum_{\varepsilon_{\tilde{v}}=\varepsilon_v} \langle v | V_{\vec{B}}^{(e)} | \tilde{v} \rangle \langle \tilde{v} c | I''(\omega) | cv \rangle \langle \tilde{v} | V_{\text{HFS}}^{(\mu)} | v' \rangle \Big), \quad (31)
\end{aligned}$$

$$\begin{aligned}
I_{\mu}^{(3c)} = & \sum_{\varepsilon_c=\varepsilon_{1s}} \left(\sum_{n_1, n_2}^{(\varepsilon_{n_1} \neq \varepsilon_v, \varepsilon_{n_2} \neq \varepsilon_c)} \frac{2}{(\varepsilon_v - \varepsilon_{n_1})(\varepsilon_c - \varepsilon_{n_2})} \left[\langle v | V_{\vec{B}}^{(e)} | n_1 \rangle \langle c | V_{\text{HFS}}^{(\mu)} | n_2 \rangle \langle n_1 n_2 | I(0) | v' c \rangle \right. \right. \\
& + \langle v | V_{\vec{B}}^{(e)} | n_1 \rangle \langle n_1 c | I(0) | v' n_2 \rangle \langle n_2 | V_{\text{HFS}}^{(\mu)} | c \rangle + \langle v | V_{\text{HFS}}^{(\mu)} | n_1 \rangle \langle c | V_{\vec{B}}^{(e)} | n_2 \rangle \langle n_1 n_2 | I(0) | v' c \rangle \\
& + \langle v | V_{\text{HFS}}^{(\mu)} | n_1 \rangle \langle n_1 c | I(0) | v' n_2 \rangle \langle n_2 | V_{\vec{B}}^{(e)} | c \rangle \Big] \\
& + \sum_{n_1, n_2}^{(\varepsilon_{n_1} \neq \varepsilon_c, \varepsilon_{n_2} \neq \varepsilon_c)} \frac{2}{(\varepsilon_c - \varepsilon_{n_1})(\varepsilon_c - \varepsilon_{n_2})} \left[\langle c | V_{\vec{B}}^{(e)} | n_1 \rangle \langle n_1 | V_{\text{HFS}}^{(\mu)} | n_2 \rangle \langle n_2 v | I(0) | cv' \rangle \right. \\
& + \langle c | V_{\vec{B}}^{(e)} | n_1 \rangle \langle n_1 v | I(0) | n_2 v' \rangle \langle n_2 | V_{\text{HFS}}^{(\mu)} | c \rangle + \langle c | V_{\text{HFS}}^{(\mu)} | n_1 \rangle \langle n_1 | V_{\vec{B}}^{(e)} | n_2 \rangle \langle n_2 v | I(0) | cv' \rangle \Big] \\
& - \sum_{\varepsilon_{\tilde{c}}=\varepsilon_{1s}} \sum_n^{(\varepsilon_n \neq \varepsilon_c)} \frac{2}{(\varepsilon_c - \varepsilon_n)^2} \left[\langle c | V_{\vec{B}}^{(e)} | n \rangle \langle n | V_{\text{HFS}}^{(\mu)} | \tilde{c} \rangle \langle \tilde{c} v | I(0) | cv' \rangle \right. \\
& \left. + \langle c | V_{\vec{B}}^{(e)} | n \rangle \langle nv | I(0) | \tilde{c} v' \rangle \langle \tilde{c} | V_{\text{HFS}}^{(\mu)} | c \rangle + \langle c | V_{\vec{B}}^{(e)} | \tilde{c} \rangle \langle \tilde{c} | V_{\text{HFS}}^{(\mu)} | n \rangle \langle nv | I(0) | cv' \rangle \right], \quad (32)
\end{aligned}$$

$$\begin{aligned}
I_{\mu}^{(3d)} = & - \sum_{\varepsilon_c=\varepsilon_{1s}} \left(\sum_{n_1, n_2}^{(\varepsilon_{n_1} \neq \varepsilon_v, \varepsilon_{n_2} \neq \varepsilon_c)} \frac{2}{(\varepsilon_v - \varepsilon_{n_1})(\varepsilon_c - \varepsilon_{n_2})} \left[\langle v | V_{\vec{B}}^{(e)} | n_1 \rangle \langle c | V_{\text{HFS}}^{(\mu)} | n_2 \rangle \langle n_1 n_2 | I(\omega) | cv' \rangle \right. \right. \\
& + \langle v | V_{\vec{B}}^{(e)} | n_1 \rangle \langle n_1 c | I(\omega) | n_2 v' \rangle \langle n_2 | V_{\text{HFS}}^{(\mu)} | c \rangle + \langle v | V_{\text{HFS}}^{(\mu)} | n_1 \rangle \langle c | V_{\vec{B}}^{(e)} | n_2 \rangle \langle n_1 n_2 | I(\omega) | cv' \rangle \\
& \left. \left. + \langle v | V_{\text{HFS}}^{(\mu)} | n_1 \rangle \langle n_1 c | I(\omega) | n_2 v' \rangle \langle n_2 | V_{\vec{B}}^{(e)} | c \rangle \right] \right. \\
& + \sum_{n_1, n_2}^{(\varepsilon_{n_1} \neq \varepsilon_c, \varepsilon_{n_2} \neq \varepsilon_c)} \frac{2}{(\varepsilon_c - \varepsilon_{n_1})(\varepsilon_c - \varepsilon_{n_2})} \left[\langle c | V_{\vec{B}}^{(e)} | n_1 \rangle \langle n_1 | V_{\text{HFS}}^{(\mu)} | n_2 \rangle \langle n_2 v | I(\omega) | v' c \rangle \right. \\
& + \langle c | V_{\vec{B}}^{(e)} | n_1 \rangle \langle n_1 v | I(\omega) | v' n_2 \rangle \langle n_2 | V_{\text{HFS}}^{(\mu)} | c \rangle + \langle c | V_{\text{HFS}}^{(\mu)} | n_1 \rangle \langle n_1 | V_{\vec{B}}^{(e)} | n_2 \rangle \langle n_2 v | I(\omega) | v' c \rangle \\
& - \sum_{\varepsilon_{\tilde{c}}=\varepsilon_{1s}} \sum_n^{(\varepsilon_n \neq \varepsilon_c)} \frac{2}{(\varepsilon_c - \varepsilon_n)^2} \left[\langle c | V_{\vec{B}}^{(e)} | n \rangle \langle n | V_{\text{HFS}}^{(\mu)} | \tilde{c} \rangle \langle \tilde{c} v | I(\omega) | v' c \rangle \right. \\
& + \langle c | V_{\vec{B}}^{(e)} | n \rangle \langle n v | I(\omega) | v' \tilde{c} \rangle \langle \tilde{c} | V_{\text{HFS}}^{(\mu)} | c \rangle + \langle c | V_{\vec{B}}^{(e)} | \tilde{c} \rangle \langle \tilde{c} | V_{\text{HFS}}^{(\mu)} | n \rangle \langle n v | I(\omega) | v' c \rangle \\
& - \sum_{\varepsilon_{\tilde{c}}=\varepsilon_{1s}} \sum_n^{(\varepsilon_n \neq \varepsilon_c)} \frac{2}{\varepsilon_c - \varepsilon_n} \left[\langle c | V_{\vec{B}}^{(e)} | n \rangle \langle n | V_{\text{HFS}}^{(\mu)} | \tilde{c} \rangle \langle \tilde{c} v | I'(\omega) | v' c \rangle \right. \\
& + \langle c | V_{\vec{B}}^{(e)} | n \rangle \langle n v | I'(\omega) | v' \tilde{c} \rangle \langle \tilde{c} | V_{\text{HFS}}^{(\mu)} | c \rangle + \langle c | V_{\vec{B}}^{(e)} | \tilde{c} \rangle \langle \tilde{c} | V_{\text{HFS}}^{(\mu)} | n \rangle \langle n v | I'(\omega) | v' c \rangle \\
& - \sum_{\varepsilon_{\tilde{c}}=\varepsilon_{1s}} \sum_n^{(\varepsilon_n \neq \varepsilon_v)} \frac{2}{\varepsilon_v - \varepsilon_n} \left[\langle v | V_{\vec{B}}^{(e)} | n \rangle \langle n c | I'(\omega) | \tilde{c} v' \rangle \langle \tilde{c} | V_{\text{HFS}}^{(\mu)} | c \rangle + \langle v | V_{\text{HFS}}^{(\mu)} | n \rangle \langle n c | I'(\omega) | \tilde{c} v' \rangle \langle \tilde{c} | V_{\vec{B}}^{(e)} | c \rangle \right] \\
& + \sum_{\varepsilon_{\tilde{v}}=\varepsilon_v} \sum_n^{(\varepsilon_n \neq \varepsilon_c)} \frac{2}{\varepsilon_c - \varepsilon_n} \left[\langle v | V_{\vec{B}}^{(e)} | \tilde{v} \rangle \langle \tilde{v} c | I'(\omega) | n v' \rangle \langle n | V_{\text{HFS}}^{(\mu)} | c \rangle + \langle v | V_{\text{HFS}}^{(\mu)} | \tilde{v} \rangle \langle \tilde{v} c | I'(\omega) | n v' \rangle \langle n | V_{\vec{B}}^{(e)} | c \rangle \right] \\
& - \sum_{\varepsilon_{\tilde{v}}=\varepsilon_v} \sum_{\varepsilon_{\tilde{c}}=\varepsilon_{1s}} \left[\langle v | V_{\vec{B}}^{(e)} | \tilde{v} \rangle \langle \tilde{v} c | I''(\omega) | \tilde{c} v' \rangle \langle \tilde{c} | V_{\text{HFS}}^{(\mu)} | c \rangle + \langle v | V_{\text{HFS}}^{(\mu)} | \tilde{v} \rangle \langle \tilde{v} c | I''(\omega) | \tilde{c} v' \rangle \langle \tilde{c} | V_{\vec{B}}^{(e)} | c \rangle \right] \\
& + \sum_{\varepsilon_{\tilde{c}}=\varepsilon_{1s}} \sum_{\varepsilon_{\tilde{c}}=\varepsilon_{1s}} \langle c | V_{\vec{B}}^{(e)} | \tilde{c} \rangle \langle \tilde{c} v | I''(\omega) | v' \tilde{c} \rangle \langle \tilde{c} | V_{\text{HFS}}^{(\mu)} | c \rangle \Big). \tag{33}
\end{aligned}$$

Here

$$\langle n_1 n_2 | I(\omega) | n_3 n_4 \rangle \equiv \int d\vec{x}_1 d\vec{x}_2 u_{n_1}^\dagger(\vec{x}_1) u_{n_2}^\dagger(\vec{x}_2) I(\omega) u_{n_3}(\vec{x}_1) u_{n_4}(\vec{x}_2), \tag{34}$$

$$I(\omega) = \alpha \frac{(1 - \vec{\alpha}_1 \cdot \vec{\alpha}_2) \cos(\omega r_{12})}{r_{12}}, \tag{35}$$

$$I'(\omega) = \frac{dI(\omega)}{d\omega}, \quad I''(\omega) = \frac{d^2 I(\omega)}{d\omega^2}, \tag{36}$$

$$\omega = \varepsilon_v - \varepsilon_{1s}, \text{ and } r_{12} = |\vec{x}_1 - \vec{x}_2|.$$

For checking purposes the corresponding calculation of the function $B_\mu(\alpha Z)$ was performed in the Coulomb gauge as well. The results of both calculations coincide with each other.

4 Numerical results

In Table 1, we present the numerical results for the function $S_2(\alpha Z)$. The exact values calculated for the point-like and extended nuclear charge distribution models are presented in the fourth and fifth columns, respectively.

In Table 2, we present the numerical results for the function $B_\mu(\alpha Z)$ defined by Eq. (28),

$$B_\mu(\alpha Z) = B_\mu^{(a)}(\alpha Z) + B_\mu^{(b)}(\alpha Z) + B_\mu^{(c)}(\alpha Z) + B_\mu^{(d)}(\alpha Z), \quad (37)$$

for the $2s$ state. $B_\mu^{(a)}(\alpha Z)$, $B_\mu^{(b)}(\alpha Z)$, $B_\mu^{(c)}(\alpha Z)$, and $B_\mu^{(d)}(\alpha Z)$ denote contributions from the corresponding diagrams presented in Fig. 3. All the values are calculated for the extended nuclear charge distribution. The root-mean-square nuclear charge radii were taken from [43]. For those elements for which no accurate experimental radii were available we employed the empirical expression [44]

$$\langle r^2 \rangle^{1/2} = 0.836A^{1/3} + 0.570(\pm 0.05) \text{ fm}, \quad (38)$$

where A is the nuclear mass expressed in a.m.u.

The dual kinetic balance (DKB) approach to basis-set expansion for the Dirac equation [45] was used for these calculations. The basis DKB functions were constructed from B-splines [46, 47]. The Fermi model was used for the nuclear charge distribution. The uncertainties were estimated by adding quadratically two errors, one obtained by varying $\langle r^2 \rangle^{1/2}$ within its uncertainty and the other obtained by changing the model of the nuclear-charge distribution from the Fermi to the homogeneously-charged-sphere model.

5 Discussion

The total $2s$ g -factor value of a lithiumlike ion with nonzero nuclear spin can be represented by

$$\begin{aligned} g &= (g_D + \Delta g_{\text{int}} + \Delta g_{\text{QED}} + \Delta g_{\text{rec}}^{(e)} + \Delta g_{\text{NS}} + \Delta g_{\text{NP}})Y_{\text{el}}(F) \\ &\quad - \frac{m_e}{m_p}(g_I + \Delta g_{\text{rec}}^{(n)})Y_{\text{nuc}}^{(\mu)}(F) + \delta g_{\text{HFS}(\mu)}^{(2s)} + \delta g_{\text{HFS}(Q)}^{(2s)}, \end{aligned} \quad (39)$$

where

$$Y_{\text{el}}(F) = \frac{F(F+1) + 3/4 - I(I+1)}{2F(F+1)} = \begin{cases} -\frac{1}{2I+1} & \text{for } F = I - \frac{1}{2} \\ \frac{1}{2I+1} & \text{for } F = I + \frac{1}{2} \end{cases}, \quad (40)$$

$Y_{\text{nuc}}^{(\mu)}(F)$ is defined by equation (16). The individual contributions to the g factor of the ground state of some Li-like ions are presented in Table 3 for $F = I - 1/2$ and in Table 4 for $F = I + 1/2$. The Dirac point-nucleus value is obtained by Eq. (8). The interelectronic-interaction (Δg_{int}), QED (Δg_{QED}), nuclear-recoil ($\Delta g_{\text{rec}}^{(e)}$), and nuclear-size (Δg_{NS}) corrections are obtained as described in Refs. [36, 37]. To estimate the nuclear-polarization correction to the g factor of Li-like ions with nonzero nuclear spin, we used the corresponding values for the zero-nuclear-spin isotopes [18] with the 100% uncertainty. This correction is essential only for heavy elements. Since in all the cases under consideration the absolute value of the recoil correction $\Delta g_{\text{rec}}^{(n)}$ to the bound-nucleus g factor is smaller than 10^{-11} [11], it is omitted in Tables 3 and 4.

The hyperfine-interaction corrections $\delta g_{\text{HFS}(\mu)}^{(2s)}$ and $\delta g_{\text{HFS}(Q)}^{(2s)}$ are given by formulas (14) and (15), respectively. The uncertainty due to uncalculated second- and higher-order terms in Eq.

(14) was estimated as the first-order correction ($\sim B_\mu(\alpha Z)/Z$) multiplied by the factor $2/Z$. The uncertainty due to uncalculated first- and higher-order terms in Eq. (15) was estimated in a similar way.

It can be seen from Tables 3 and 4 that, as a rule, the electric-quadrupole hyperfine-interaction correction is much smaller than the magnetic-dipole one. This is due to an additional factor $(\alpha Z)^2$ in formula (15) compared to formula (14) and small values of Q for low- Z ions. However, in case of $^{235}\text{U}^{89+}$ these corrections are of the same order of magnitude.

The uncertainties of the nuclear magnetic moments indicated in Tables 3 and 4, as a rule, do not include errors due to unknown chemical shifts which, in some cases, can contribute on the level of a few tenths percents. This means that measurements of the g factor with the aforementioned accuracy could provide the most accurate determinations of the nuclear magnetic moments. The hyperfine-interaction correction evaluated in this paper will be important for this determination.

Acknowledgements

D.L.M. thanks N.S. Oreshkina for valuable advice. He is also grateful to GSI. This work was supported by INTAS-GSI (Grant No. 05-111-4937). V.M.S. acknowledges the support by INTAS-GSI grant No. 06-1000012-8881.

References

- [1] N. Hermanspahn, H. Häffner, H.-J. Kluge, W. Quint, S. Stahl, J. Verdú, and G. Werth, Phys. Rev. Lett. **84** (2000) 427.
- [2] H. Häffner, T. Beier, N. Hermanspahn, H.-J. Kluge, W. Quint, S. Stahl, J. Verdú, and G. Werth, Phys. Rev. Lett. **85**, 5308 (2000).
- [3] J.L. Verdú, S. Djekić, S. Stahl, T. Valenzuela, M. Vogel, G. Werth, T. Beier, H.-J. Kluge, W. Quint, Phys. Rev. Lett. **92**, 093002 (2004).
- [4] S.A. Blundell, K.T. Cheng, J. Sapirstein, Phys. Rev. A **55**, 1857 (1997).
- [5] H. Persson, S. Salomonson, P. Sunnergren, and I. Lindgren, Phys. Rev. A **56**, R2499 (1997).
- [6] T. Beier, I. Lindgren, H. Persson, S. Salomonson, P. Sunnergren, H. Häffner, and N. Hermanspahn, Phys. Rev. A **62**, 032510 (2000).
- [7] A. Czarnecki, K. Melnikov, and A. Yelkhovsky, Phys. Rev. A **63**, 012509 (2001).
- [8] S.G. Karshenboim, in *The Hydrogen Atom*, edited by S.G. Karshenboim *et al.* (Springer, Berlin, 2001), p. 651.
- [9] S. Karshenboim, V.G. Ivanov, and V.M. Shabaev, Can. J. Phys. **79**, 81 (2001); Zh. Eksp. Teor. Fiz. **120**, 546 (2001) [JETP **93**, 477 (2001)].
- [10] V.M. Shabaev, Phys. Rev. A **64**, 052104 (2001).
- [11] A.P. Martynenko and R.N. Faustov, Zh. Eksp. Teor. Fiz. **120**, 539 (2001) [JETP **93**, 471 (2001)].

- [12] D.A. Glazov and V.M. Shabaev, Phys. Lett. A **297**, 408 (2002).
- [13] T. Beier, H. Häffner, N. Hermanspahn, S.G. Karshenboim, H.-J. Kluge, W. Quint, S. Stahl, J. Verdú, and G. Werth, Phys. Rev. Lett. **88**, 011603 (2002).
- [14] V.M. Shabaev and V.A. Yerokhin, Phys. Rev. Lett. **88**, 091801 (2002).
- [15] V.A. Yerokhin, P. Indelicato, and V.M. Shabaev, Phys. Rev. Lett. **89**, 143001 (2002).
- [16] V.M. Shabaev, D.A. Glazov, M.B. Shabaeva, V.A. Yerokhin, G. Plunien, and G. Soff, Phys. Rev. A **65**, 062104 (2002).
- [17] V.A. Yerokhin, P. Indelicato, and V.M. Shabaev, Phys. Rev. A **69**, 052503 (2004).
- [18] A.V. Nefiodov, G. Plunien, and G. Soff, Phys. Rev. Lett. **89**, 081802 (2002).
- [19] S.G. Karshenboim and V.G. Ivanov, Can. J. Phys. **80**, 1305 (2002).
- [20] D. L. Moskovkin, N. S. Oreshkina, V. M. Shabaev, T. Beier, G. Plunien, W. Quint, and G. Soff, Phys. Rev. A **70**, 032105 (2004).
- [21] D. L. Moskovkin and V. M. Shabaev, Phys. Rev. A **73**, 052506 (2006).
- [22] P.J. Mohr and B.N. Taylor, Rev. Mod. Phys. **77**, 1 (2005).
- [23] G. Werth, H. Häffner, N. Hermanspahn, H.-J. Kluge, W. Quint, J. Verdú, in *The Hydrogen Atom*, edited by S.G. Karshenboim *et al.* (Springer, Berlin, 2001), p. 204.
- [24] V.M. Shabaev, D.A. Glazov, N.S. Oreshkina, A.V. Volotka, G. Plunien, H.-J. Kluge, and W. Quint, Phys. Rev. Lett. **96**, 253002 (2006).
- [25] V.M. Shabaev, Can. J. Phys. **76**, 907 (1998).
- [26] V.M. Shabaev, Phys. Rep. **356**, 119 (2002).
- [27] S.M. Schneider, W. Greiner, and G. Soff, Z. Phys. **31**, 143 (1994).
- [28] H. Winter, S. Borneis, A. Dax, S. Faber, T. Kühl, F. Schmitt, P. Seelig, W. Seelig, V.M. Shabaev, M. Tomaselli, M. Würtz, in : GSI Scientific Report 1998, edited by U. Grundinger, (GSI, Darmstadt, 1999), p. 87.
- [29] R.A. Hegstrom, Phys. Rev. A **11**, 421 (1975).
- [30] L. Veseth, Phys. Rev. A **22**, 803 (1980).
- [31] E. Lindroth and A. Ynnerman, Phys. Rev. A **47**, 961 (1993).
- [32] Z.-C. Yan, Phys. Rev. Lett. **86**, 5683 (2001).
- [33] Z.-C. Yan, J. Phys. B **35**, 1885 (2002).
- [34] P. Indelicato, E. Lindroth, T. Beier, J. Bieron, A.M. Costa, I. Lindgren, J.P. Marques, A.-M. Martensson-Pendrill, M.C. Martins, M.A. Ourdane, F. Parente, P. Patte, G.S. Rodrigues, S. Salomonson, and J.P. Santos, Hyperfine Interact. **132**, 349 (2001).

- [35] V.M. Shabaev, D.A. Glazov, M.B. Shabaeva, I.I. Tupitsyn, V.A. Yerokhin, T. Beier, G. Plunien, and G. Soff, Nuclear Instruments and Methods in Physics Research B 205 (2003) 20-24.
- [36] D.A. Glazov, V.M. Shabaev, I.I. Tupitsyn, A.V. Volotka, V.A. Yerokhin, G. Plunien, and G. Soff, Phys. Rev. A **70**, 062104 (2004).
- [37] D.A. Glazov, A.V. Volotka, V.M. Shabaev, I.I. Tupitsyn, G. Plunien, Phys. Lett. A **357** (2006) 330-333.
- [38] V.M. Shabaev, O.V. Andreev, A.N. Artemyev, S.S. Baturin, A.A. Elizarov, Y.S. Kozhedub, N.S. Oreshkina, I.I. Tupitsyn, V.A. Yerokhin, and O.M. Zherebtsov, International Journal of Mass Spectrometry 251 (2006) 109-118.
- [39] W. Quint, J. Dilling, S. Djekić, H. Häffner, N. Hermanspahn, H.-J. Kluge, G. Marx, R. Moore, D. Rodriguez, J. Schönfelder, G. Sikler, T. Valenzuela, J. Verdú, C. Weber, and G. Werth, Hyperfine Interactions **132**, 453 (2001).
- [40] H.A. Bethe, E.E. Salpeter, *Quantum mechanics of one and two electron atoms*, Springer, Berlin, 1957.
- [41] B. Sz.-Nagy, Comm. Mat. Helv. **19**, 347 (1946/47); T. Kato, Progr. Theor. Phys. **4**, 514 (1949); **5**, 95 (1950); **5**, 207 (1950).
- [42] V.M. Shabaev, in *Many-Party Effects in Atoms*, edited by U.I. Safronova (AN SSSR, Nauchnyj Sovet po Spektroskopii, 1988), p. 15; Izv. VUZ Fiz. **33**, 43 (1990) [Sov. Phys. J. **33**, 660 (1990)].
- [43] I. Angeli, At. Data Nucl. Data Tables **87**, 185 (2004).
- [44] W.R. Johnson and G. Soff, At. Data Nucl. Data Tables **33**, 405 (1985).
- [45] V.M. Shabaev, I.I. Tupitsyn, V.A. Yerokhin, G. Plunien, and G. Soff, Phys. Rev. Lett. **93**, 130405 (2004).
- [46] W.R. Johnson and J. Sapirstein, Phys. Rev. Lett. **57**, 1126 (1986).
- [47] W.R. Johnson, S.A. Blundell, and J. Sapirstein, Phys. Rev. A **37**, 307 (1988).
- [48] P. Raghavan, At. Data Nucl. Data Tables **42**, 189(1989).
- [49] P. Pykkö, Mol. Phys. **99**, 1617 (2001).

Table 1: Numerical results for the function $S_2(\alpha Z)$ defined by Eq. (18). S_2^{point} is the point-nucleus value obtained by formula (20). S_2^{ext} is the extended-nucleus value. The values of $\langle r^2 \rangle^{1/2}$ are taken from Ref. [43].

Ion	Z	$\langle r^2 \rangle^{1/2}$ (fm)	$S_2^{\text{point}}(\alpha Z)$	$S_2^{\text{ext}}(\alpha Z)$
${}^7\text{Li}$	3	2.431	1.00076	1.00076
${}^9\text{Be}^+$	4	2.518	1.00136	1.00136
${}^{11}\text{B}^{2+}$	5	2.406	1.00212	1.00212
${}^{13}\text{C}^{3+}$	6	2.461	1.00306	1.00306
${}^{14}\text{N}^{4+}$	7	2.558	1.00417	1.00417
${}^{17}\text{O}^{5+}$	8	2.695	1.00545	1.00545
${}^{19}\text{F}^{6+}$	9	2.898	1.00691	1.00691
${}^{21}\text{Ne}^{7+}$	10	2.967	1.00855	1.00854
${}^{33}\text{S}^{13+}$	16	3.251	1.02224	1.02218
${}^{43}\text{Ca}^{17+}$	20	3.493	1.03527	1.03513
${}^{53}\text{Cr}^{21+}$	24	3.659	1.05171	1.05145
${}^{67}\text{Zn}^{27+}$	30	3.964	1.08359	1.08296(1)
${}^{73}\text{Ge}^{29+}$	32	4.063	1.09637	1.09555(2)
${}^{91}\text{Zr}^{37+}$	40	4.284	1.16037	1.15824(3)
${}^{113}\text{In}^{46+}$	49	4.602	1.26402	1.25820(6)
${}^{115}\text{In}^{46+}$	49	4.617	1.26402	1.25818(6)
${}^{119}\text{Sn}^{47+}$	50	4.645	1.27819	1.27170(7)
${}^{127}\text{I}^{50+}$	53	4.750	1.32460	1.31566(9)
${}^{129}\text{Xe}^{51+}$	54	4.776	1.34148	1.33156(10)
${}^{131}\text{Xe}^{51+}$	54	4.781	1.34148	1.33155(10)
${}^{143}\text{Nd}^{57+}$	60	4.923	1.46042	1.4420(2)
${}^{159}\text{Tb}^{62+}$	65	5.060	1.58862	1.5577(8)
${}^{173}\text{Yb}^{67+}$	70	5.304	1.75329	1.7004(3)
${}^{177}\text{Hf}^{69+}$	72	5.333	1.83238	1.7674(4)
${}^{185}\text{Re}^{72+}$	75	5.329	1.96892	1.8806(6)
${}^{187}\text{Re}^{72+}$	75	5.339	1.96892	1.8805(6)
${}^{195}\text{Pt}^{75+}$	78	5.428	2.13172	2.0095(7)
${}^{197}\text{Au}^{76+}$	79	5.436	2.19299	2.0570(7)
${}^{199}\text{Hg}^{77+}$	80	5.448	2.25827	2.1068(8)
${}^{207}\text{Pb}^{79+}$	82	5.494	2.40235	2.2136(10)
${}^{209}\text{Bi}^{80+}$	83	5.521	2.48199	2.2709(10)
${}^{229}\text{Th}^{87+}$	90	5.681	3.23718	2.764(3)
${}^{231}\text{Pa}^{88+}$	91	5.700	3.38354	2.850(3)
${}^{235}\text{U}^{89+}$	92	5.829	3.54308	2.935(2)
${}^{257}\text{Fm}^{97+}$	100	5.886	5.57470	3.870(7)

Table 2: The contributions to the interelectronic-interaction correction $B_\mu(\alpha Z)$, defined by Eq. (28), from the diagrams presented in Figs. 3–5. The values of $\langle r^2 \rangle^{1/2}$ are given in Table 1.

Ion	Z	$B_\mu^{(a)}(\alpha Z)$	$B_\mu^{(b)}(\alpha Z)$	$B_\mu^{(c)}(\alpha Z)$	$B_\mu^{(d)}(\alpha Z)$	$B_\mu(\alpha Z)$
${}^7\text{Li}$	3	-1.45058	-0.0588955	-0.230825	0.146787	-1.59351
${}^9\text{Be}^+$	4	-1.45215	-0.0591841	-0.231117	0.147153	-1.59529
${}^{11}\text{B}^{2+}$	5	-1.45417	-0.0595557	-0.231493	0.147625	-1.59759
${}^{13}\text{C}^{3+}$	6	-1.45664	-0.0600107	-0.231953	0.148205	-1.60040
${}^{14}\text{N}^{4+}$	7	-1.45957	-0.0605498	-0.232499	0.148894	-1.60373
${}^{17}\text{O}^{5+}$	8	-1.46296	-0.0611736	-0.233130	0.149694	-1.60757
${}^{19}\text{F}^{6+}$	9	-1.46682	-0.0618828	-0.233850	0.150607	-1.61194
${}^{21}\text{Ne}^{7+}$	10	-1.47114	-0.0626786	-0.234657	0.151636	-1.61684
${}^{33}\text{S}^{13+}$	16	-1.50734(1)	-0.0693364(4)	-0.241442(1)	0.160434(1)	-1.65769(1)
${}^{43}\text{Ca}^{17+}$	20	-1.54187(1)	-0.0756850(2)	-0.247960(1)	0.169119(2)	-1.69639(1)
${}^{53}\text{Cr}^{21+}$	24	-1.58556(2)	-0.0837272(8)	-0.256270(2)	0.180504(4)	-1.74505(2)
${}^{67}\text{Zn}^{27+}$	30	-1.67053(4)	-0.099395(3)	-0.272617(4)	0.203796(9)	-1.83874(3)
${}^{73}\text{Ge}^{29+}$	32	-1.70468(4)	-0.105707(4)	-0.279253(6)	0.21355(1)	-1.87609(4)
${}^{91}\text{Zr}^{37+}$	40	-1.87649(9)	-0.13762(1)	-0.31312(1)	0.26566(3)	-2.06157(9)
${}^{113}\text{In}^{46+}$	49	-2.1556(2)	-0.19021(3)	-0.36966(3)	0.35919(5)	-2.3563(2)
${}^{115}\text{In}^{46+}$	49	-2.1556(2)	-0.19021(3)	-0.36965(3)	0.35917(5)	-2.3563(2)
${}^{119}\text{Sn}^{47+}$	50	-2.1938(2)	-0.19748(3)	-0.37751(3)	0.37268(7)	-2.3961(2)
${}^{127}\text{I}^{50+}$	53	-2.3186(2)	-0.22141(4)	-0.40340(5)	0.41789(9)	-2.5255(3)
${}^{129}\text{Xe}^{51+}$	54	-2.3640(3)	-0.23017(4)	-0.41287(5)	0.43469(9)	-2.5724(3)
${}^{131}\text{Xe}^{51+}$	54	-2.3640(3)	-0.23016(4)	-0.41287(5)	0.43468(9)	-2.5723(3)
${}^{143}\text{Nd}^{57+}$	60	-2.6825(5)	-0.29243(8)	-0.48024(8)	0.5574(2)	-2.8977(3)
${}^{159}\text{Tb}^{62+}$	65	-3.021(2)	-0.3603(3)	-0.5535(4)	0.6961(8)	-3.239(2)
${}^{173}\text{Yb}^{67+}$	70	-3.4456(9)	-0.4477(2)	-0.6470(2)	0.8792(4)	-3.6612(10)
${}^{177}\text{Hf}^{69+}$	72	-3.647(2)	-0.4900(2)	-0.6919(2)	0.9690(5)	-3.8597(12)
${}^{185}\text{Re}^{72+}$	75	-3.990(2)	-0.5632(3)	-0.7692(4)	1.1257(6)	-4.196(2)
${}^{187}\text{Re}^{72+}$	75	-3.989(2)	-0.5632(3)	-0.7691(4)	1.1256(6)	-4.196(2)
${}^{195}\text{Pt}^{75+}$	78	-4.383(2)	-0.6494(4)	-0.8591(4)	1.3116(8)	-4.580(2)
${}^{197}\text{Au}^{76+}$	79	-4.529(2)	-0.6818(4)	-0.8927(4)	1.3819(9)	-4.722(3)
${}^{199}\text{Hg}^{77+}$	80	-4.683(3)	-0.7162(5)	-0.9282(5)	1.4565(10)	-4.870(3)
${}^{207}\text{Pb}^{79+}$	82	-5.013(3)	-0.7912(5)	-1.0052(7)	1.6196(12)	-5.189(3)
${}^{209}\text{Bi}^{80+}$	83	-5.191(4)	-0.8322(5)	-1.0469(7)	1.7089(13)	-5.361(3)
${}^{229}\text{Th}^{87+}$	90	-6.738(9)	-1.2047(16)	-1.417(2)	2.520(4)	-6.840(9)
${}^{231}\text{Pa}^{88+}$	91	-7.011(11)	-1.2732(17)	-1.484(2)	2.669(5)	-7.099(9)
${}^{235}\text{U}^{89+}$	92	-7.279(7)	-1.3429(13)	-1.5499(15)	2.819(4)	-7.353(7)
${}^{257}\text{Fm}^{97+}$	100	-10.26(3)	-2.156(5)	-2.301(5)	4.558(12)	-10.16(2)

Table 3: The individual contributions to the ground-state g factor of lithiumlike ions with nonzero nuclear spin for $F = I - \frac{1}{2}$. The values of $\langle r^2 \rangle^{1/2}$ are given in Table 1. The values of I , $\frac{\mu}{\mu_N}$, and Q are given in Table 4.

Ion	$^{17}\text{O}^{5+}$	$^{33}\text{S}^{13+}$	$^{43}\text{Ca}^{17+}$	$^{53}\text{Cr}^{21+}$
$g_{\text{D}}Y_{\text{el}}(F)$	-0.333238563	-0.499429548	-0.249553251	-0.498709516
$\Delta g_{\text{int}}Y_{\text{el}}(F)$	-0.000029443(5)	-0.00009031(2)	-0.000056806(18)	-0.00013712(5)
$\Delta g_{\text{QED}}Y_{\text{el}}(F)$	-0.000386592(2)	-0.000580176(15)	-0.000290213(13)	-0.00058076(4)
$\Delta g_{\text{rec}}^{(e)}Y_{\text{el}}(F)$	-0.000000003	-0.000000011(1)	-0.000000007	-0.000000017(1)
$\Delta g_{\text{NS}}Y_{\text{el}}(F)$	0.0	-0.000000001	-0.000000002	-0.000000009
$-\frac{m_e}{m_p}g_I Y_{\text{nuc}}^{(\mu)}(F)$	0.00048132(2)	-0.000292197(1)	0.000230660(1)	0.00021537(1)
$\delta g_{\text{HFS}(\mu)}^{(2s)}$	-0.000000014(1)	0.000000019	-0.000000019	-0.000000022
$\delta g_{\text{HFS}(Q)}^{(2s)}$	0.0	0.0	0.0	0.0
g	-0.33317330(2)	-0.50039222(3)	-0.24966964(2)	-0.49921208(7)

Ion	$^{73}\text{Ge}^{29+}$	$^{131}\text{Xe}^{51+}$	$^{209}\text{Bi}^{80+}$	$^{235}\text{U}^{89+}$
$g_{\text{D}}Y_{\text{el}}(F)$	-0.199075231	-0.493187551	-0.193006882	-0.238840328
$\Delta g_{\text{int}}Y_{\text{el}}(F)$	-0.00007397(4)	-0.0003249(3)	-0.0002175(3)	-0.0003127(5)
$\Delta g_{\text{QED}}Y_{\text{el}}(F)$	-0.00023270(2)	-0.00058679(11)	-0.00024077(13)	-0.0003049(2)
$\Delta g_{\text{rec}}^{(e)}Y_{\text{el}}(F)$	-0.000000009(1)	-0.000000040(15)	-0.00000003(4)	-0.00000004(9)
$\Delta g_{\text{NS}}Y_{\text{el}}(F)$	-0.000000016	-0.000000839(3)	-0.000008752(17)	-0.00002999(6)
$\Delta g_{\text{NP}}Y_{\text{el}}(F)$	—	—	—	0.00000003(3)
$-\frac{m_e}{m_p}g_I Y_{\text{nuc}}^{(\mu)}(F)$	0.000117082	-0.000314000(2)	-0.00054724(3)	0.000068(12)
$\delta g_{\text{HFS}(\mu)}^{(2s)}$	-0.000000017	0.000000097	0.000000445	-0.000000080(14)
$\delta g_{\text{HFS}(Q)}^{(2s)}$	0.0	0.000000001	0.000000002	-0.000000046(1)
g	-0.19926487(4)	-0.4944140(3)	-0.1940207(3)	-0.239420(12)

Table 4: The individual contributions to the ground-state g factor of lithiumlike ions with nonzero nuclear spin for $F = I + \frac{1}{2}$. The values of $\langle r^2 \rangle^{1/2}$ are given in Table 1. The values of $\frac{\mu}{\mu_N}$ and Q are taken from Refs. [48] and [49], respectively.

Ion	$^{13}\text{C}^{3+}$	$^{17}\text{O}^{5+}$	$^{33}\text{S}^{13+}$	$^{43}\text{Ca}^{17+}$
I	1/2	5/2	3/2	7/2
μ/μ_N	0.7024118(14)	-1.89379(9)	0.6438212(14)	-1.317643(7)
Q (barn)	—	-0.02558(22)	-0.0678(13)	-0.0408(8)
$g_{\text{D}}Y_{\text{el}}(F)$	0.999840150	0.333238563	0.499429548	0.249553251
$\Delta g_{\text{int}}Y_{\text{el}}(F)$	0.000065379(10)	0.000029443(5)	0.00009031(2)	0.000056806(18)
$\Delta g_{\text{QED}}Y_{\text{el}}(F)$	0.001159708(3)	0.000386592(2)	0.000580176(15)	0.000290213(13)
$\Delta g_{\text{rec}}^{(e)}Y_{\text{el}}(F)$	0.000000005(1)	0.000000003	0.000000011(1)	0.000000007
$\Delta g_{\text{NS}}Y_{\text{el}}(F)$	0.0	0.0	0.000000001	0.000000002
$-\frac{m_e}{m_p}g_I Y_{\text{nuc}}^{(\mu)}(F)$	-0.000382545(1)	0.000343797(16)	-0.000175318	0.000179403(1)
$\delta g_{\text{HFS}(\mu)}^{(2s)}$	0.000000007(1)	-0.000000010(1)	0.000000011	-0.000000015
$\delta g_{\text{HFS}(Q)}^{(2s)}$	—	0.0	0.0	0.0
g	1.000682704(10)	0.333998387(17)	0.49992474(3)	0.25007967(2)

Ion	$^{53}\text{Cr}^{21+}$	$^{73}\text{Ge}^{29+}$	$^{129}\text{Xe}^{51+}$	$^{131}\text{Xe}^{51+}$
I	3/2	9/2	1/2	3/2
μ/μ_N	-0.47454(3)	-0.8794677(2)	-0.7779763(84)	0.6918619(39)
Q (barn)	-0.150(50)	-0.196	—	-0.114(1)
$g_{\text{D}}Y_{\text{el}}(F)$	0.498709516	0.199075231	0.986375103	0.493187551
$\Delta g_{\text{int}}Y_{\text{el}}(F)$	0.00013712(5)	0.00007397(4)	0.0006497(6)	0.0003249(3)
$\Delta g_{\text{QED}}Y_{\text{el}}(F)$	0.00058076(4)	0.00023270(2)	0.0011736(2)	0.00058679(11)
$\Delta g_{\text{rec}}^{(e)}Y_{\text{el}}(F)$	0.000000017(1)	0.000000009(1)	0.000000008(3)	0.000000040(15)
$\Delta g_{\text{NS}}Y_{\text{el}}(F)$	0.000000009	0.000000016	0.000001678(5)	0.000000839(3)
$-\frac{m_e}{m_p}g_I Y_{\text{nuc}}^{(\mu)}(F)$	0.000129221(8)	0.000095795	0.000423699(5)	-0.000188400(1)
$\delta g_{\text{HFS}(\mu)}^{(2s)}$	-0.000000013	-0.000000014	-0.000000130	0.000000058
$\delta g_{\text{HFS}(Q)}^{(2s)}$	0.0	0.0	—	0.0
g	0.49955663(7)	0.19947771(4)	0.9886237(6)	0.4939117(3)

Table 4 (*continued*)

Ion	$^{207}\text{Pb}^{79+}$	$^{209}\text{Bi}^{80+}$	$^{235}\text{U}^{89+}$
I	1/2	9/2	7/2
μ/μ_N	0.59258(1)	4.1106(2)	-0.39(7) ^a
Q (barn)	—	-0.516(15)	4.936(6)
$g_{\text{D}}Y_{\text{el}}(F)$	0.966001452	0.193006882	0.238840328
$\Delta g_{\text{int}}Y_{\text{el}}(F)$	0.0010703(14)	0.0002175(3)	0.0003127(5)
$\Delta g_{\text{QED}}Y_{\text{el}}(F)$	0.0012023(7)	0.00024077(13)	0.0003049(2)
$\Delta g_{\text{rec}}^{(e)}Y_{\text{el}}(F)$	0.00000013(18)	0.00000003(4)	0.00000004(9)
$\Delta g_{\text{NS}}Y_{\text{el}}(F)$	0.00003921(8)	0.000008752(17)	0.00002999(6)
$\Delta g_{\text{NP}}Y_{\text{el}}(F)$	-0.00000002(2)	—	-0.00000003(3)
$-\frac{m_e}{m_p}g_IY_{\text{nuc}}^{(\mu)}(F)$	-0.000322731(5)	-0.00044774(2)	0.000053(10)
$\delta g_{\text{HFS}(\mu)}^{(2s)}$	0.000000253	0.000000364	-0.000000062(11)
$\delta g_{\text{HFS}(Q)}^{(2s)}$	—	-0.000000001	0.000000021(1)
g	0.9679909(15)	0.1930266(3)	0.239541(10)

^a An average of the values given in Ref. [48].

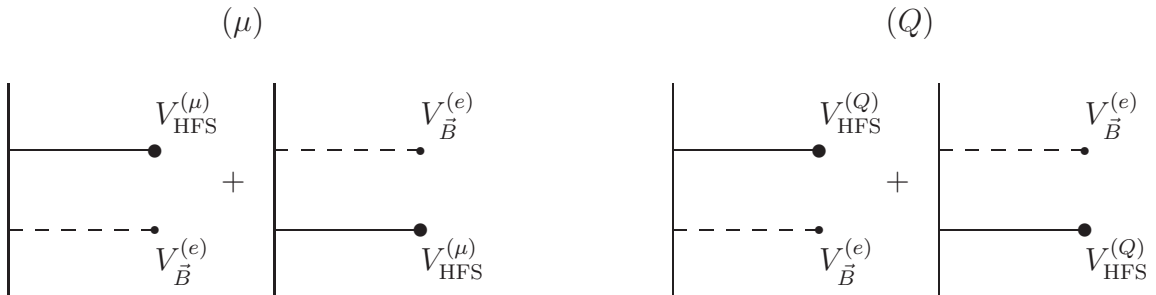


Figure 1: The second-order diagrams contributing to $\delta g_{\text{HFS}}^{(2s)}$.

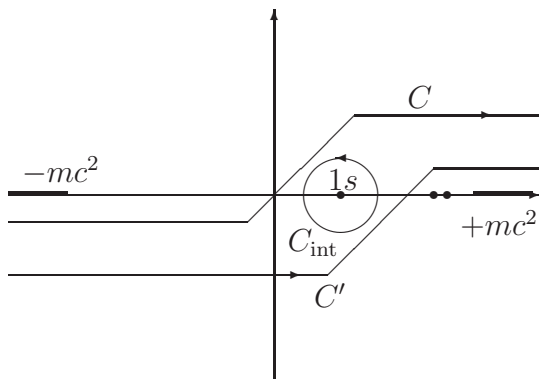


Figure 2: C is the original contour of the integration over the electron energy variable in the formalism with the standard vacuum. C' is the integration contour for the vacuum with the $(1s)^2$ shell included. The integral along the contour $C_{\text{int}} = C' - C$ describes the interaction of the valent electron with the $(1s)^2$ -shell electrons.

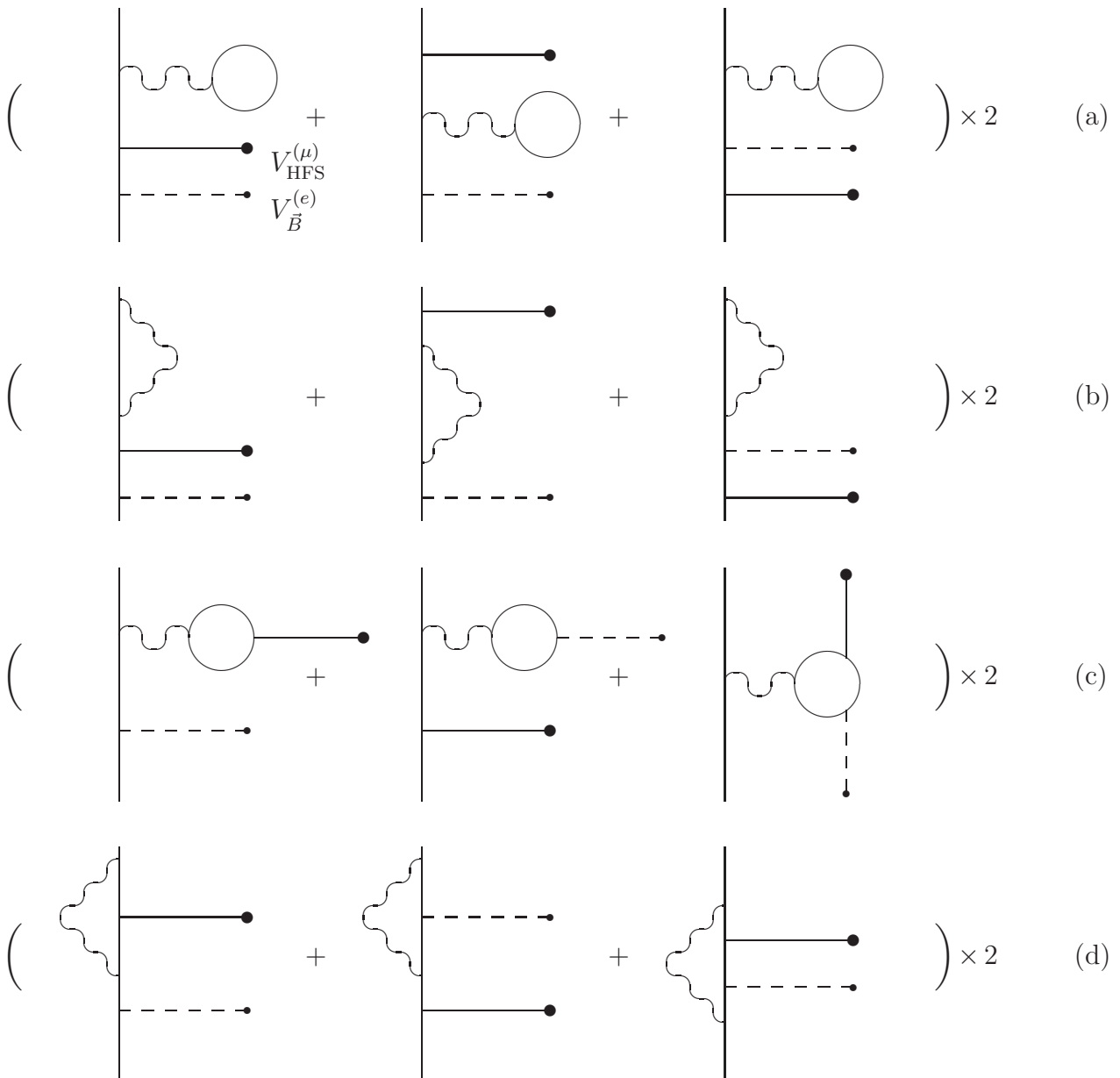


Figure 3: The third-order diagrams contributing to $\delta g_{\text{HFS}(\mu)}^{(2s)}$.

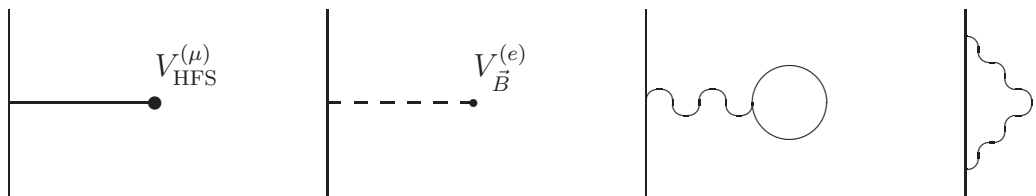


Figure 4: The first-order diagrams contributing to $\delta g_{\text{HFS}(\mu)}^{(2s)}$ being multiplied by the second-order diagrams presented in Fig. 5.

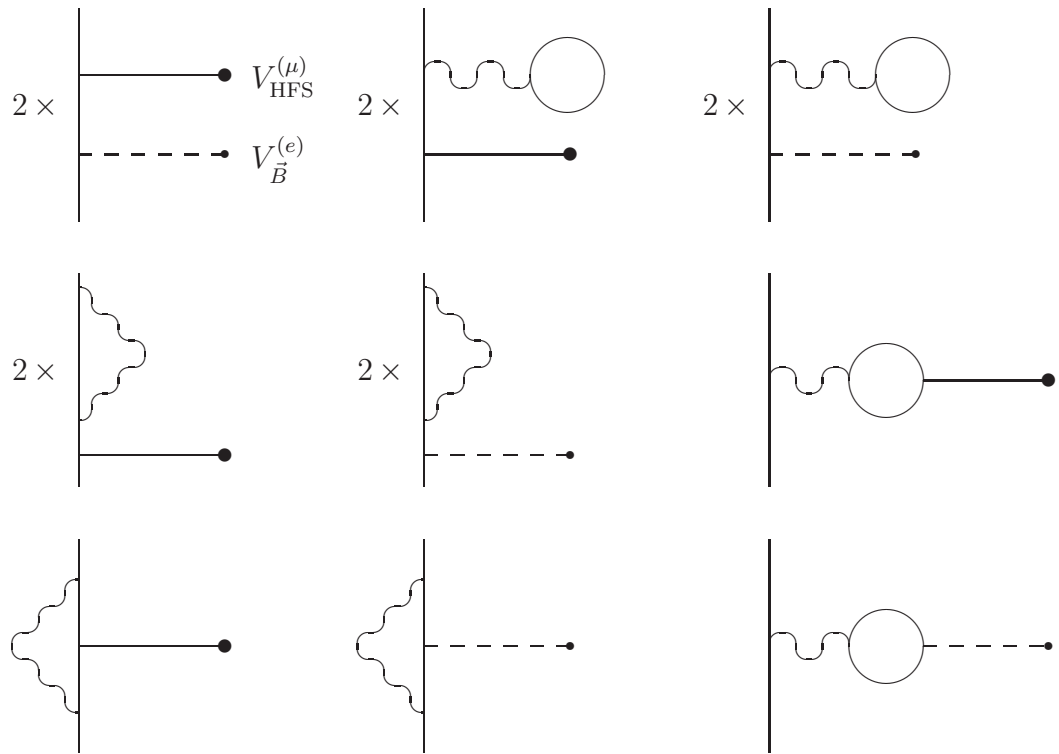


Figure 5: The second-order diagrams contributing to $\delta g_{\text{HFS}(\mu)}^{(2s)}$ being multiplied by the first-order diagrams presented in Fig. 4.